Phase Equilibrium and Optimization Tools: Application for Enhanced Structured Lipids for Foods

Moises Teles dos Santos [a,b,c], Galo A.C. Le Roux [a], Vincent Gerbaud [b,c]*

[a] *Universidade de São Paulo, Escola Politécnica, Laboratório de Simulação e Controle de Processos, Av. Prof. Lineu Prestes, São Paulo,5088-900 BRASIL*

[b] *Université de Toulouse, INP, UPS, LGC (Laboratoire de Génie Chimique), 4 allée Emile Monso, F-31432 Toulouse Cedex 04 – France*

[c] *CNRS, LGC (Laboratoire de Génie Chimique), F-31432 Toulouse Cedex 04 – France*

* corresponding author: Vincent.Gerbaud@ensiacet.fr

Abstract

Solid-liquid phase equilibrium modeling of triacylglycerols mixtures is essential for lipids design. Considering the α polymorphism and liquid phase as ideal, the Margules 2-suffix excess Gibbs energy model with predictive binary parameter correlations describes the non ideal β and β' solid polymorphs. Solving by direct optimization of the Gibbs free energy enables to predict from a bulk mixture composition the phases composition at a given temperature and thus the SFC curve, the melting profile and the Differential Scanning Calorimetry (DSC) curve that are related to end-user lipid properties. Phase diagram, SFC and DSC curve experimental data are qualitatively and quantitatively well predicted for the binary mixture 1,3-dipalmitoyl-2-oleoyl-*sn*-glycerol (POP) and 1,2,3-tripalmitoyl-*sn*-glycerol (PPP), the ternary mixture 1,3-dimyristoyl-2-palmitoyl-*sn*-glycerol (MPM), 1,2-distearoyl-3-oleoyl-*sn*-glycerol (SSO) and 1,2,3-trioleoyl-*sn*-glycerol (OOO), for palm oil and cocoa butter. Then, addition to palm oil of Medium-Long-Medium type structured lipids is evaluated, using caprylic acid as medium chain and long chain fatty acids (EPA-eicosapentaenoic acid, DHA-docosahexaenoic acid, γ-linolenic-octadecatrienoic acid and AA-arachidonic acid), as sn-2 substitutes. EPA, DHA and AA increase the melting range on both the fusion and crystallization side. γ-linolenic shifts the melting range upwards. This predictive tool is useful for the pre-screening of lipids matching desired properties set *a priori*.

Keywords: triacylglycerols, structured lipids, solid-liquid equilibrium, DSC, Solid Fat Content, melting point, medium chain fatty acid, long chain fatty acid.

Symbols

ΔH	enthalpy (kJ/mol)	Subscripts	
ε	Degree of isomorphism	*i*	component i
γ	activity coefficient	*o*	pure state

μ	chemical potential (kJ/mol)	m	melting state
a	Binary interaction parameter	Superscripts	
A	Binary interaction parameter	j	solid phase j
Cp	molar heat capacity (kJ/mol)	nc	number of components
G	extensive Gibbs free energy (kJ)	np	number of phases
g	molar Gibbs free energy (kJ/mol)	E	excess property
$\bar{g}$	partial molar Gibbs free energy (kJ/mol)	ap	apparent
H	extensive enthalpy (kJ)	p	phase p
n	number of mols		
P	pressure (bar)		
q	Molecule size parameter		
R	gas constant (kJ/mol.K)		
S	specific entropy (kJ/mol.K)		
T	temperature (K)		
V	molar volume (cm^3/mol)		
v_0	Sum of the carbon number		
V_{non}	Absolute difference in carbon number		
x	molar fraction		

Introduction

The so-called functional foods represent an expanding market and food functionalizing is a major factor driving the development of new products [1]. Fat-based foods are composed mainly by triacylglycerols (TAGs), a class of lipids responsible for more than 95% of composition in fats and oils. Such molecules have a large application in the food industry: they are important sources of energy, essential fatty acids, fat-soluble vitamins and they impart flavor, texture and palatability to foods [2]. When determining the suitability of novel lipids for use in food application, physico-chemical properties of fat-based products such as improved spreadability, a specific melting point, a particular solid fat content (SFC) at a given temperature, melting profiles (SFC curves), precise rheological behavior and crystal habit are as fundamental as texture, appearance or nutritional properties [3]. Acknowledging the expertise of food makers, matching these physico-chemical end-user properties often remains an empirical recipe in practice and more systematic (computer-based approaches) as we consider in this manuscript, can be useful for evaluate triacylglycerols mixtures in a pre-experimental step.

Bulk physiochemical properties and sensory attributes of many fatty foods are determined by the fraction of the fat phase that is solidified at a particular temperature, namely the SFC curve [4]. Fat based food products used as bakery shortenings enhancer can be described mainly by 7 sensory attributes: color, texture, moistness, oiliness, denseness,

taste and aroma and principal component analysis showed that color, SFC, melting temperature, aroma and denseness are the main factors enabling to discriminate among products [5].

Taste is strongly correlated with melting temperature and SFC perception in mouth [3,5]: fats should be completely melted at 36°C and SFC contributes to the cooling sensations of a product in the mouth. In margarines, a large difference between the SFC at 15°C and 25°C is correlated to increased cooling sensations [3]. In baking shortening, optimal performance is achieved with SFC between 15% and 25% at usage temperature whereas an excess of liquid can cause oiliness sensation decreasing scores of sensorial attributes [5].

Considering available experimental information, phase diagrams, differential scanning calorimetry (DSC) curves, SFC melting curves and fatty acid distributions are found, bringing information of various interest. Rarely found fat phase diagrams report the clear and softening points. The clear point is the temperature at which the last solid phase disappears (completely fusion) and the softening point is the temperature at which the last liquid phase disappears (complete crystallization). On the other hand, DSC curves are often a readily available measurement that can display solid phase transitions; quite clearly for simple TAGs or fatty acid systems but hardly readable for oils.

The fat complete melting point gives limited information of the fat consistency. Indeed, fats with the same final melting point can have widely different consistency at room temperature. On the other hand, a SFC curve describes the whole melting profile of a fat and can also be correlated with sensory attributes such as hardness [6,7].

The fatty acid distribution is often measured but it is not straightforward to relate it to the SFC and therefore to end-user properties. A reason is that oils are mixtures of triacylglycerols, with each of the triacylglycerol (TAG) bearing three fatty acids, and that each TAG can crystallize in several polymorphic forms, each with its own melting point.

So-called Structured Lipids (SLs) are defined as lipids restructured by chemical or enzymatic processes to change their fatty acid composition and/or the stereochemical positions of fatty acids on the glycerol backbone. Among the possible improvements sought are specific metabolic effects, nutritive or therapeutic purposes, physical and/or chemical characteristics of lipids [8]. MLM (medium-long-medium) and CLA (conjugated

linoleic acids) triacylglycerols are recognized for their improved nutritional characteristics [9]. MLM has medium chain fatty acids (MCFA) (C6-C12) in stereo positions sn-1 and sn-3 of the glycerol backbone and functional long-chain polyunsaturated fatty acids (PUFA) in position sn-2. The CLA is a general term for the positional and geometric isomers of octadecadienoic acid with conjugated double bonds at carbon atoms 9/11 or 10/12 [9].

MLM molecules utilize the benefits of the fast energy provided by the medium-chain fatty acid (specially caprylic, capric, caproic and lauric acids) and the nutritional effects of long-chain fatty acid, especially EPA (5,8,11,14,17-eicosapentaenoic acid – C20:5), DHA (4,7,10,13,16,19-docosahexaenoic acid – C22:6), γ- linolenic acid (6,9,12-octadecatrienoic acid – C18:3) and AA (arachidonic acid – C20:4) [9].

MCFA have several desired features such as high oxidative stability (due to their saturation), low viscosity and melting points and high solubility in water. They also provide quick energy and fast absorption without significant tendency to accumulate in the fat tissues [8]. As MCFA alone cannot provide essential fatty acids, they are combined with long chain fatty acids (LCFA) for better nutritional purposes, not achieved by physical mixture of long chain and medium chain fatty acids [10].

The LCFA, like the famous omega-3, polyunsaturated fatty acids have been recognized for their important role in health: EPA can reduce the level of very low density lipoprotein (VLDL) and low-density lipoprotein (LDL) cholesterol in humans and can help to prevent arteriosclerosis and thrombosis. DHA is important for brain development and retina [11,12].

Therefore, positioning medium-chain fatty acids in the sn-1 and sn-3 position of the glycerol backbone imparts fast absorption of these acids in the body while unsaturated long-chain fatty acids in the sn-2 position may increase the nutritional value of the molecules involved.

The number of possible tailor-made TAGs rapidly increases with the number of fatty acids considered (see Fig.1), as different sets composed by 3 fatty acids can be used and, for a given set, many positional isomers can be formed. Together with the consideration of the final mixture composition and number of TAGs present as variables, the problem size becomes impossible to handle experimentally.

Insert figure 1 here

The present work concerns the validation of a predictive solid-liquid equilibrium algorithm by direct minimization of Gibbs Free Energy. It enables to evaluate how molecular structure and mixture composition affect final properties such as SFC and melting profiles suitable for hinting at the recipe directions that must be investigated to achieve enhanced chemical structures for nutritional purposes while satisfying consumers sensorial requirements. This work fits in our scope of computer aided product design (CAPD) for structured lipids where target properties of various kinds (SLE-related properties like here, nutritious power, viscosity properties,etc..) are set as the objective of a reverse engineering problem and many candidate mixtures of oils and value added TAGs are evaluated by predictive tools with respect to these target properties [13].

First the solid – liquid equilibrium principles are described in the light of TAGs application and former modeling works are recalled before selecting a model suitable for a predictive tool. Second, the solving scheme based on optimization is presented along with a synthesis of robustness and numerical issues. Third, the predictive model is validated, without any fitting, on selected systems for which experimental data is available, first on binary and ternary TAGs mixtures, then on multi-component vegetable oils (palm oil and cocoa butter). Finally, structured lipids for which there are no experimental data as mixtures of palm oil supplemented with value-added MLM TAGs are considered, in order to investigate how the added TAG affects their melting curves. Table 1 summarizes the mixtures used in this work.

Insert table 1 here

Methods

Background on fat thermodynamic equilibrium modeling

Due to their high molecular weight, TAGs tend to crystallize in a solid network with different crystals packing called polymorphisms. The most common are the unstable α-form (least dense crystal packing), the metastable β'-form and the stable β-form (most dense crystal packing) [14]. Polymorphic forms are distinguished by their own

temperature of fusion and enthalpy of fusion and they impact SFC and DSC curves which are indeed used experimentally to explore the polymorphic behavior of fats.

SFC computation until 1990 was mainly empirical, partially based on curve fitting [15]. After 1990, the literature mostly published experimental studies [16-18] and some equilibrium modeling issues [19, 20-22]. Won [20] used iterative methods to compute softening and clear points with no considerations about computing activity coefficients on solid and liquid phases and applied it to cocoa butter.

There are mainly three solid-liquid equilibrium models that have been used in the current literature for fatty mixtures: Bragg–Williams approximation [23], Slaughter and Doherty model [24] and Margules-isomorphism correlations [15,19]. Bragg–Williams approximation assumes non-ideal mixing in both liquid and solid phases and attributes the non-ideality of mixing to the enthalpy term of the free energy of mixing, supposing that the entropy term is like in the ideal mixing. It uses parameters which are the energy difference between molecules pairs in solid and liquid phases, fitted to experimental binary data [25,26]. Slaughter and Doherty model deals with solid compound-forming systems, like stoichiometric peritectic compound in the solid phase and considers that the solid phases are almost immiscible. Seven binary fatty acid mixtures were also studied with Slaughter and Doherty model for the solid phase while testing Margules-2-suffix, Margules-3-suffix, UNIFAC modified Dortmund 93, and NRTL thermodynamic excess Gibbs free energy models to compute the liquid activity coefficients [22]. Fitting those model parameters to experimental data, the authors concluded that the combination of the Slaughter–Doherty model for solid and Margules-3-suffix model for liquids achieved the best reproduction of the experimental data. Concerning the Margules-isomorphism model, a large experimental data collection was examined and noticed that Margules interaction parameters in the β' and β solid phases were reasonably correlated to the degree of isomorphism between 2 molecules [15]. Application of Flory Huggins theory led them to consider the liquid phase as ideal in most cases, except when large difference in molecular size (differences in carbon number greater than 15-20) occurs among the TAGs [15]. Besides they concluded that solid non ideality comes from substantial distortion in the regular crystal lattice of a pure component by adding a molecule of

another size and that distortion is non significant in a disordered state as α polymorph but must be accounted for the denser packed β' and β systems.

After analysis of these previous works, we selected the Margules model [27] in the present work, as it is well-suited for mixtures whose components have similar molar volumes, shape and chemical nature . Also, the isomorphism correlation for the Margules binary interaction parameters will be used because they serve to our goal of running predictive simulations without fitting any parameter on experimental data within the context of CAPD reverse formulation.

Despite the occurrence of other fat solid polymorphism such as γ and of sub-forms such as $\beta 2$ and $\beta 3$ [15], we only consider the α, β and β' solid phases possibly in equilibrium with a liquid phase, as there are no predictive models to calculate melting temperature and melting enthalpy in other forms and experimental data are very scarce.

The Margules model and the isomorphism correlations are detailed in appendix A.

Solid –liquid equilibrium modeling of fats

The condition for thermodynamic equilibrium is that the chemical potential of each component i in each phase must be equal to that in any other phase. For a liquid phase in equilibrium with at least one solid phase j,

$$\mu_i^{liquid} = \mu_i^{solid(j)} \tag{1}$$

or

$$\mu_{i,0}^{liquid} + RT\,ln(\gamma_i^{liquid} x_i^{liquid}) = \mu_{i,0}^{solid(j)} + RT\,ln(\gamma_i^{solid(j)} x_i^{solid(j)}) \tag{2}$$

For the chemical potential of molecule i in the reference state:

$$d\mu_{i,0}^{p} = -S_{i,0}^{p} dT + V_{i,0}^{p} dP \tag{3}$$

where:

$$\Delta S_{i,0} = \Delta H_{i,0} / T \text{ and } \Delta H_{i,0} = \Delta H_{m,i,0} + \Delta Cp_{i,0}(T - T_{m,i}) \tag{4}$$

The effect of pressure in condensed phases such as solids and liquid can be neglected at pressures not too high. Assuming ΔCp_i to be independent of temperature, after some rearrangements Equation (1) can be rewritten as:

$$ln\left(\frac{\gamma_i^{solid(j)} x_i^{solid(j)}}{\gamma_i^{liquid} x_i^{liquid}}\right) = \frac{\Delta H_{m,i}^{solid(j)}}{R}\left(\frac{1}{T} - \frac{1}{T_{m,i}^{solid(j)}}\right) - \frac{\Delta C_{p,i}}{R}\left(\frac{T_{m,i}^{solid(j)} - T}{T}\right) + + \frac{\Delta C_{p,i}}{R} ln\frac{T_{m,i}^{solid(j)}}{T} \quad (5)$$

Solid – liquid equilibrium can also be formulated in terms of Gibbs free energy that must be minimal at equilibrium. The intensive Gibbs free energy for a phase *p* is:

$$g^p = \sum_{i=1}^{nc} x_i^p (\mu_{i,0}{}^p + RT \ln \gamma_i^p x_i^p) \quad (6)$$

For TAG systems ΔCp = 0.2 kJ/mol and the difference (T_m – T) is never greater than 70K (usually between 0-20) [15]. Together with setting the chemical potential in the pure liquid reference state to zero, this enables to simplify Eq.(6) and write for the liquid phase molar Gibbs free energy:

$$g^{liquid} = RT \sum_{i=1}^{nc} (x_i^{liquid} \ln x_i^{liquid}) \quad (7)$$

and for *p* being one of the possible solid phases (α, β' or β):

$$g^p = RT \sum_{i=1}^{nc} x_i^p \left(\frac{\Delta H_{m,i}^p}{R}\left(\frac{1}{T} - \frac{1}{T_{m,i}^p}\right) + \ln \gamma_i^p x_i^p\right) \quad (8)$$

Solving the solid – liquid equilibrium by direct minimization of Gibbs Free Energy

Computing phase equilibrium is the solution of a nonlinear programming problem searching for the global minimization of the Gibbs Free Energy G, subject to material balance constraints written as an equivalent set of nonlinear equations:

$$\begin{aligned} &\min G(n) = \sum_{i=1}^{nc}\sum_{j=1}^{np} n_i^j \mu_i^j(n) = \sum_{j=1}^{np} n^j g^j \\ &s.t. \\ &n_i = \sum_{j=1}^{np} n_i^j \quad i = 1 \ldots nc \\ &0 \le n_i^j \le n_i \;\; i = 1 \ldots nc;\; j = 1 \ldots np \end{aligned} \quad (9)$$

The solution of the solid liquid equilibrium gives the number of phases, the fraction of each phase and their composition. When spanning a temperature range, the total solid content, SFC and DSC curves can be computed.

One of the main difficulties associated with minimizing the Gibbs free energy is the *a priori* determination of the number of phases. If too few phases are allowed, then

convergence to constrained minima can occur; if too many are assumed, then numerical problems may arise like Jacobian matrix singularities in Newton-based methods, or convergence to trivial or local extrema may occur [28]. In a previous work, we succeeded to solve the SLE for several 9 TAGs mixtures in a two step approach: first solving the stability tests and second computing the equilibrium compositions [29]. The Michelsen's method [30] for stability analysis was adapted to cope with polymorphisms and was successful for phase-split detection but revealed to be initialization dependent and failed in detecting phase split for some mixtures. To overcome this limitation, the present work deals with direct minimization of Gibbs Free Energy using a Generalized Reduced Gradient (GRG) method available in the GAMS software [31] considering a priori a sufficient number of phases to be present, namely 9 solid phases plus a liquid in our case. After some initial evaluations of the performance of the available optimizers, one has chosen CONOPT3 among six others as it showed the best relation time / accuracy in finding exact solutions for selected mixtures of known results. Solving 10 times the palm oil example with 17 TAGs over 79 temperatures (2370 optimization problems) was achieved in 31 seconds with 0/79 failures. The second best available optimizer based on a branch-and-cut method, had a mean failure of 8/79 and required more than a 300 times more time, whereas its accuracy in terms of minimum Gibbs free energy value was 0.01% higher than those obtained with CONOPT3.

To summarize the calculation section, the bulk mixture composition in TAGs is an input as well as the temperature of calculation. Then 9 solid phases + 1 liquid phases are supposed initially to co-exists with TAGs splitted randomly between the initial phases. The Gibbs free energy optimization predicts the number of coexisting phases and their TAG composition along with their Gibbs free energy value and the total Gibbs free energy value. The SFC curve is then readily computed from this information by sequentially increasing the temperature of the mixture until there is no more solid present.

Differential scanning calorimetry curve simulation

A DSC curve is related to apparent heat capacity which can be computed from the following equations [32]:

$$C_p^{ap} = C_p + \left(\frac{\partial H}{\partial T}\right)_n \qquad (10)$$

Also, the Excess enthalpy and Excess Gibbs energy are given by:

$$H^E = H - \sum_{j=1}^{np}\sum_{i=1}^{nc} n_i^j H_{i,0}^j \quad (11)$$

$$G^E = H^E - TS^E \quad (12)$$

Setting reference enthalpy to zero on liquid state, H_0 for any i specie on phase j in equation 11 becomes the melting enthalpy of that solid phase. Thus:

$$H_{i,0}^j = \Delta H_{m,i}^j \quad (13)$$

Assuming that triacylglycerols solid mixtures are regular solutions (excess entropy equals to zero), $H^E = G^E$ and an expression for H can be put from equation 11 into equation 10 to compute the apparent heat capacity taking into account the solid transitions:

$$C_p{}^{ap} = C_p + \frac{\partial G^E}{\partial T} + \sum_{j=1}^{np}\sum_{i=1}^{nc} \Delta H_{m,i}^j \frac{\partial n_i{}^j}{\partial T} \quad (14)$$

Equation 14 shows that for each point on the DSC curve, the apparent heat capacity can be calculated by using two derivatives, which in turn can be obtained by numerical differentiation of SLE results (Excess Gibbs energy and number of moles) at two different temperatures (Ti and Ti + ΔT).

The DSC simulated curves are then calculated with the hypothesis that chemical equilibrium has been reached; which may rarely be the case for all experimental DSC curves that are cooling/heating rates dependent.

Pure component properties needed for computing SFC curves from SLE are the melting temperature (Tm), the melting enthalpy (Hm) to which is added the heat capacity (Cp) for DSC curves. Whenever possible, the experimental data bank for Tm and Hm for different polymorphism for different TAGs was used [15]. But in the context of CAPD reverse formulation, we have also used temperature and enthalpy of fusion correlations based on carbon number, number of double bounds, position of fatty acids in the molecule and asymmetry [15] or a group interaction contribution model for saturated TAGs that accounts for isomerism [33]. For heat capacity, we used a recent published group contribution method regressed over 1395 values for 86 types of fatty compounds (saturated and unsaturated FA, fatty esters, fatty alcohols, saturated and unsaturated

TAGs and hydrocarbons) [34]. The reader should consult the references cited for further details.

Results and Discussions

Binary mixture (Palmitic-Oleic-Palmitic/ Palmitic- Palmitic- Palmitic)

Solid-liquid T,x,y phase diagram experimental data [35] for the binary mixture Palmitic-Oleic-Palmitic (POP) and Palmitic- Palmitic- Palmitic (PPP) are compared in Fig.2 with the simulated results. The TAGs crystals are in the β form (no submodifications β1 or β2 of the β class are considered in this work). The solid line (softening points) and liquid line (clear points) with a large region of coexistence solid-liquid for the whole range of POP fraction can be seen.

Insert figure 2 here

Predictions agree better with the liquid phase line than with the solid phase line, especially for POP-lean mixtures. Although deceptive, these results are in accordance with previous literature results [15]: according to those authors, this is related to the fact that the visual observations of clear and specially softening points are very inaccurate. Also, impurities can increase the melting points and incomplete stabilization due to extremely low diffusion rates in solid phase can lead to imprecision in determine the initial temperature of fusion and thus the solid phase line location.

In the POP-rich region, the increasing presence of the unsaturated oleic chain, well known for its very low melting point near 14°C, lowers the TAG mixture melting range.

Ternary Mixture (Myristic-Palmitic-Myristic/Stearic-Stearic-Oleic/Oleic-Oleic-Oleic)

The SFC-temperature curve is computed for the ternary-mixture Myristic-Palmitic-Myristic (MPM), Stearic-Stearic-Oleic (SSO) and Oleic-Oleic-Oleic (OOO) with mass composition 25%, 25% and 50% respectively (Fig.3a). Then the DSC curve is computed from equations (14) and compared in Fig.3b with experimental data in the β' modification obtained at 1.25°C/min after a 3 day stabilization time [15]. They are in good quantitative and qualitative agreement.

Insert figure 3 here

In this mixture, the triolein (OOO) TAG (melting point -10°C), is used as a “liquid solvent” to increase the diffusion rates of MPM and SSO in solid phase. The model correctly detected that at the start temperature of 17°C all the OOO TAG (50% of the mixture composition) is in the liquid phase, in agreement with the experimental observation It must be highlighted that at the initial temperature, the computer tool randomly distribute the molecules in the phases, and then the solver converges to a solution. In the MPM/SSO/OOO case, despite an initial random amount of OOO in solid phase being non-zero, the method correctly converged to zero amount of solid OOO.

The DSC curve displays two peaks. The first one is the endothermic peak caused by fusion of SSO (experimental T_m=41.9ºC) and the second one is due to the MPM fusion (experimental T_m=59.5ºC). That curve with distinct melting peaks is typical for mixtures where the molecules are well-distinguished one from another in shape and size. The low isomorphism (0.77) of such a mixture is responsible for its non ideal behavior. One also notes that the transition temperatures in the mixture (Fig.3b) do not correspond to the pure compound temperature transitions as the mixture deviates from ideal behavior.

Pure Palm Oil

Computation for palm oil is another step in the computer tool validation. Palm oil currently accounts for 13% of the total world production of oils and fats and is expected to overtake soybean oil as the most important vegetable oil. Almost 90% of the world palm oil production is used as food [36].

Insert Table 2 here

In this work, the palm oil is modeled by 17 TAGs corresponding to 91.56 % in weight of palm oil composition (Table 2). Data about the TAGs type and composition was taken from literature [36] and minor components (TAGs and other molecules) with very low fraction or not available/computed pure properties were discarded. None of these minor components are responsible for more than 0.83% of overall composition. Only the TAG explicited in table 2 were considered in the calculations, after renormalization.

Lin [37] recorded the SFC at seven temperatures for 244 samples of palm oils of various origins. The SFC computed from the renormalized composition of Table 2 is

compared to the mean experimental points [37] in Fig.4a. Fig.4b shows the related DSC simulation for this vegetable oil. We do not compare to other models for palm oil as we found no other melting range calculation by using modeling in the literature.

Insert figure 4 here

Fig.4a shows that despite some discrepancy, the SFC curve shape agrees with the experimental data: the final melting points are alike; from 10 °C to 20 ° C both simulated and experimental data display a steep slope, while from 25° C to 40° C the slope is softer. Overall, the mean difference over the 10 to 40°C range between the calculated and experimental SFC value is 8.2%. The predicted SFC curve also indicates that there is only solid at -20°C. It can also determine the solid fraction at any intermediate temperatures, giving useful information for product design requirements.

Looking at the DSC curve, its shape is typical for mixtures with a high number of molecules. The number of peaks is different from the number of molecules (17) because peaks for molecules with close transition temperatures overlap. As pointed out in the literature [38], these peaks are not easily interpretable, depend on heating/cooling rates and on entire thermal history of the sample. Experimental DSC curves are scan rate, temperature programming and stability procedure dependent (which leads to experimental curves with different shapes) and numerous thermal transitions and thermal lag can occur [38]. Thus, it is difficult to choose what experimental curve must be considered. Actually, comparing simulated DSC generated by ESL results and experimental DSC curves are not suitable, unless experimental data were judiciously conducted in order to achieve equilibrium, as in the case for Fig3b. However, simulated DSC curve reveals the heat capacity change of the sample due to state transitions, indicating the temperatures where the most accentuated changes occurs.

Cocoa Butter

Cocoa butter is the only natural fat melting sharply just below mouth temperature, leaving a clean, cool, non-greasy sensation on the palate [6]. Its unique and specific TAG composition (Table 2) is responsible for these high desired sensory properties. In chocolates, a sharp melting point is a sign of intense cooling sensations in the mouth [3]. Therefore, reducing the tail of the SFC vs temperature curve is a must sought feature in

industry to improve mouth feel in cocoa butter equivalents (CBE), cocoa butter replacer (CBR) and cocoa butter substitutes (CBS).

Cocoa butter SFC experimental data was taken from literature [20] and TAG composition was taken from another source [39]. The composition reported in Table 2 shows that 12 saturated and unsaturated TAGs are used to represent cocoa butter (97.2 % weight), discarding minor components accounting for 2.8% weight. Compositions are renormalized before calculation.

Insert figure 5 here

Fig.5 shows that the model predictions are consistent with experimental data in terms of melting profile shape, but the final melting temperature is overpredicted by more than 10°C. Overall, quantitative agreement is achieved within less than 15%, a fair value considering that we do not perform any fitting. Other causes of discrepancy are the fact that the experimental data are not obtained by the authors who provided the compositions used for the prediction; the compositions for prediction discard 2.8% in weight of the measured composition.

Comparing cocoa butter and palm oil, cocoa butter has a melting range around 30°C, half that of palm oil around 60°C. The Cocoa butter DSC predictions shows broader and less numerous peaks, corresponding to more solid-liquid molecular transitions over similar temperatures.

Prediction of Palm Oil enriched with Structured Lipids (SLs)

The aim of the present algorithm is to be used in a predictive manner and we simulate the effects of adding highly unsaturated MLM molecules on the melting profile of pure palm oil.

First, the molecule Caprylic-EPA-Caprylic (caprylic - eicosapentaenoic acid – caprylic), a structured lipid of type MLM is added to palm oil in 6 different concentrations (5, 10, 20, 30, 40 and 50%). Fig.6 represents the melting curves for these mixtures whereas Fig.7 shows the related DSC curves

Insert figure 6 here

Fig.6 shows that the addition of Caprylic-EPA-Caprylic affects strongly the palm oil melting curve even at low concentrations. Pure palm oil is solid at – 20 °C, but 5% Caprylic-EPA-Caprylic already imposes some liquid content at – 20 °C. This is expected as Caprylic-EPA-Caprylic has a very low melting point due to its five unsaturations. As Caprylic-EPA-Caprylic concentration increases, the SFC decreases significantly at – 20°C, reaching 65% SFC for 50 % of Caprylic-EPA-Caprylic. However, the benefit of lowering the SFC of palm oil is not kept for the whole melting range. Indeed, the Caprylic-EPA-Caprylic enriched curves cross the pure palm oil curve and pure palm oil becomes completely melted before the Caprylic-EPA-Caprylic enriched oil. As a whole, the enriched oils have an extended melting range on both sides, with a final melting point increased about 11°C (T_m=51°C) for all concentrations between 5 and 50%.

Fig.7 shows the DSC simulations for the enriched palm oil mixtures of Fig.6. It can be noted that the Caprylic-EPA-Caprylic enriched palm oil curves are similar whatever the concentration but are very different from the pure palm oil curve. This is expected as the chemical structure of the mixture molecules is changed but it is meaningful because a single 5% Caprylic-EPA-Caprylic concentration shifts the DSC peaks significantly. But as a whole these curves are difficult to interpret in terms of properties.

Insert figure 7 here

Now, we compare the addition of 30% of four MLM structured lipids, Caprylic – X – Caprylic, with X being a LCFA: EPA (eicosapentaenoic acid - C20:5) as before, DHA (docosahexaenoic acid - C22:6), AA (arachidonic acid – C20:4) and γ - linolenic acid (6, 9,12-octadecatrienoic acid – C18:3). Fig.8 represents the melting curves for these mixtures whereas Fig.9 shows the related DSC curves.

Insert figure 8 here

The results indicate that the structured lipids with EPA, DHA and AA lower the melting points at -20°C compared to pure palm oil, whereas the addition of γ-linolenic acid increases the melting point by +18°C. Among these 4 fatty acids, the γ- linolenic has 3 double bonds (C18:3) while EPA, DHA and AA have 5, 6 and 4 double bonds respectively, resulting in very low melting points (-54ºC, -44ºC and -49ºC, respectively).

As a result, EPA, DHA and AA are all in liquid phase at the beginning of the computation and the three relevant curves overlap. Therefore, the effect of decreasing SFC is more pronounced in the last ones. But pure palm oil still exhibits the lowest crystallization temperature. Therefore one notes that EPA, DHA and AA expand the melting range on both sides whereas γ-linolenic acid shifts up upwards.

Insert figure 9 here

Fig.9 shows the corresponding DSC simulations for the mixtures of Fig.8. As in the previous case, the shape of the curves for the palm oil mixtures + SLs are very different from that of the pure palm oil and also there are differences among them, as the chemical structure of the mixtures is different for each curve.

Conclusions and Future Works

Crystallization and melting behavior play an important role in the fat-based products acceptance and quality requirements. These phenomena are modeled using a solid – liquid equilibrium framework coping with TAG polymorphism. Following literature we consider the liquid phase and the unstable α solid phase as ideal whereas the β and β' non ideal behavior is modeled with Margules activity coefficient model where the binary interaction parameter are predicted by using an isomorphism model. Solving is done by direct minimization of Gibbs free energy using a generalized reduced gradient algorithm which robustness has been assessed.

Such a modeling has been used earlier but on simple binary or ternary mixtures and always with parameter fitting of experimental data. Within the context of computer aided product design reverse engineering of new lipid based applications, the computer tool was used in a predictive manner to compute the melting range, the solid fat content vs temperature and the DSC curve from the knowledge of the TAGs blends composition.

The tool was validated on experimental data available for a binary POP/PPP mixture, on a ternary MPM/SSO/OOO mixture, on pure palm oil and cocoa butter. There is a close qualitative agreement between predictions and experimental data available. In all cases the solid fat content quantitative agreement is achieved within 15%. It was pointed that some experimental data lacked uncertainty information, likely to exist as clear and

softening points are sometimes difficult to assess when recording phase diagrams, or as DSC curves are heating rate dependent. Concerning palm oil, no comparison with other models was possible because none was found in the literature. Then the tool was used to predict the property changes when adding caprylic acid – X – caprylic acid to pure palm oil, with X being EPA (eicosapentaenoic acid - C20:5) as before, DHA (docosahexaenoic acid - C22:6), AA (arachidonic acid – C20:4) and γ- linolenic acid(C18:3). Those structured TAGs belong to the important MLM class where the long chain fatty acids in position sn-2 may bring benefits for the health.

Results showed that the lipid addition affected the SFC and the melting range even at 5% concentration. At 30% concentration, EPA, DHA and AA expand the palm oil melting range on both sides whereas γ-linolenic acid shifts up upwards

Works in preparation are heading in two directions. First the complete prediction of SFC and melting range from the fatty acid distribution instead of the TAGs composition, with underneath the generation of the TAGs themselves, using statistical models. Second, the development of a computer aided mixture and blend design framework for finding new structured lipids coping with target property values set *a priori*. In that case, the solid – liquid equilibrium tool can be supplemented with rheological behaviour prediction model, detailed nutritional power evaluation model and many other properties that qualify a specific application.

Acknowledgments

We acknowledge the financial support received from The National Council for Scientific and Technological Development (CNPq-Brazil), Coordenação de Aperfeiçoamento de Pessoal de Nível Superior (CAPES-Brazil) and the ALFA-II-400 FIPHARIAA program (Europe).

Appendix A. Margules model and Binary Interaction Parameter models.

The definition of the activity coefficient is given by the following equation [27]:

$$RT\,ln\,\gamma_i(T,P,x) = \overline{g}_i^E = \left(\frac{\partial n g^E}{\partial n_i}\right)_{T,P,n_{j\neq i}} \qquad \text{(A1)}$$

The two-suffix Margules model for multicomponent mixtures is given by:

$$g^E = \sum_{i=1}^{nc} \sum_{j=i+1}^{nc} A_{ij} x_i x_j \quad \text{(A2)}$$

Where

$$A_{ij} = 2qa_{ij} \quad \text{(A3)}$$

The term q is a measure of the size of the molecules in the pair and a_{ij} are interaction parameters between molecules i and j. In the Margules equations is assumed that $q_i = q_j = q$ (molecules with similar size). However, it is used frequently for all sorts of mixtures, regardless the relative sizes of the different molecules [27].

The work of Wesdorp [15] showed that there is a great correlation between the degree of isomorphism (coefficient of geometrical similarity) and the parameter A_{ij}. The degree of isomorphism between two TAGs can be described by the following expression:

$$\varepsilon = 1 - \frac{v_{non}}{v_o} \quad \text{(A4)}$$

v_{non} is the sum of the absolute differences in carbon number of each of three chains and for v_0 the sum of the carbon numbers of the smallest chain on each glycerol position. Linear regression of experimentally determined A_{ij} parameters vs the calculated isomorphism as defined by Eq. A4 led to the following correlations [15]:

$$\varepsilon > 0.93 : \frac{A_{ij}^{\beta'}}{RT} = 0 \text{ (high molecular similarity, complete miscibility)} \quad \text{(A5)}$$

$$\varepsilon \leq 0.93 : \frac{A_{ij}^{\beta'}}{RT} = -19.5\varepsilon + 18.2 \quad \text{(A6)}$$

$$\varepsilon > 0.98 : \frac{A_{ij}^{\beta}}{RT} = 0 \text{ (high molecular similarity, complete miscibility)} \quad \text{(A7)}$$

$$\varepsilon \leq 0.98 : \frac{A_{ij}^{\beta}}{RT} = -35.8\varepsilon + 35.9 \quad \text{(A8)}$$

The primary value of the Margules equations lies in their ability to serve as simple empirical equations for representing experimentally determined activity coefficients with only a few constants and when, as is often the case, experimental data are scattered and scarce, they serve as an efficient tool for interpolation and extrapolation with respect to composition [27].

References

1. Jiménez-Colmenero F (2007) Healthier lipid formulation approaches in meat based functional foods. Technological options for replacement of meat fats by non-meat fats. Trends Food Sci. Technol 18 (11): 567-578.
2. Yang T, Zhang H, Mu H, Sinclair AJ, Xu X (2004) Diacylglycerols from Butterfat: Production by Glycerolysis and Short-Path Distillation and Analysis of Physical Properties. J Am Oil Chem Soc 81(10): 979-987.
3. Osborn H, Akoh C (2002) Structured Lipids-Novel Fats with Medical, Nutraceutical, and Food Applications. Comprehensive Reviews in Food Science and Food Safety *3*(1): 93-103.
4. Singh AP, McClements DJ, Marangoni AG (2004) Solid fat content determination by ultrasonic velocimetry. Food Res Int 37: 545–555.
5. Arifin N, Cheong LZ, Koh SP, Long K, Tan CP, Yusoff MSA, Aini IN, Lo SK, Lai OM (2009) Physicochemical Properties and Sensory Attributes of Medium- and Long-Chain Triacylglycerols (MLCT)-Enriched Bakery Shortening. Food Bioprocess Technol. Published on line. DOI 10.1007/s11947-009-0204-0.
6. Pantzaris TP, Basiron Y (2002) The Lauric (coconut and palmkernel) oils. In: Gunstone FD (ed) Vegetable Oils in Food Technology: Composition, Properties and Uses. Blackwell, Oxford, pp.157-202.
7. Braipson-Danthine S, Deroanne C (2004) Influence of SFC, microstructure and polymorphism on texture (hardness) of binary blends of fats involved in the preparation of industrial shortenings. Food Res Int 37:941–948.
8. Lee K, Akoh C (1998) Characterization of Enzymatically Synthesized Structured Lipids Containing Eicosapentaenoic, Docosahexaenoic, and Caprylic Acids. J Am Oil Chem Soc 75(4): 495-499.
9. Timm-Heinrich M, Nielsen NS, Xu X, Jacobsen C (2004) Oxidative stability of structured lipids containing C18:0, C18:1, C18:2, C18:3 or CLA in sn2-position – as bulk lipids and in milk drinks. Innovative Food Science and Emerging Technologies *5*(2): 249-261.
10. Iwasaki Y, Yamane T (2000) Enzymatic synthesis of structured lipids. J. Mol. Catal. B: Enzym 10(1-3): 129-140.
11. Ruxton CHS, Reed SC, Simpson MJA, Millington KJ (2004) The health benefits of omega-3 polyunsaturated fatty acids: a review of the evidence. J Hum Nutr Dietet, 17, 449–459.
12. Shahidi F (2004) Functional Foods: Their Role in Health Promotion and Disease Prevention. J. Food Sci 69(5): 146-149.
13. Gani R (2004) Chemical Product Design: challenges and opportunities. Comp Chem Eng 28 2441-2457.
14. Sato K (2001) Crystallization behaviour of fats and lipids - a review. Chem. Eng. Sci 56: 2255 – 2265.
15. Wesdorp LH, van Meeteren JA, de Jong S, Giessen RVD, Overbosch P, Grootscholten PAM, Struik M, Royers E, Don A, de Loos TH, Peters C, Gandasasmita I (2005) Liquid-Multiple Solid Phase Equilibria in Fats: Theory and Experiments. In: Marangoni AG (ed) Fat Crystal Networks. New York, pp.481-710.
16. Inoue T, Hisatsugu Y, Yamamoto R, Suzuki M (2004) Solid–liquid phase behavior of binary fatty acid mixtures 1. Oleic acid/stearic acid and oleic acid/behenic acid mixtures. Chem. Phys. Lipids 127: 143–152.
17. Zhou Y, Hartel RW (2006) Phase Behavior of Model Lipid Systems: Solubility of High-Melting Fats in Low-Melting Fats. J. Am. Oil Chem. Soc 83: 505–511.
18. Zhang L, Ueno S, Miura S, Sato K (2007) Binary Phase Behavior of 1,3-Dipalmitoyl-2-oleoyl-sn-glycerol and 1,2-Dioleoyl-3-palmitoyl-rac-glycerol. J. Am. Oil Chem. Soc 84: 219 – 227.
19. Himawan C, Starov V, Stapley A (2006) Thermodynamic and kinetic aspects of fat crystallization. Adv. Colloid Interface Sci 122(1-3): 3-33.
20. Won K (1993) Thermodynamic Model of Liquid-Solid Equilibria for Natural Fats and Oils. Fluid Phase Equilibr 82: 261-273.

21. Slaughter DW, Doherty MF (1995) Calculation of solid-liquid equilibrium and crystallization paths for melt crystallization processes. Chem. Eng. Sci 50(11): 1679-1694.
22. Costa MC, Rolemberg MP, Boros LAD, Krahenbuhl MA, de Oliveira MG, Meirelles AJA (2007) Solid-Liquid Equilibrium of Binary Fatty Acid Mixtures. J.Chem.Eng. Data 52:30-36.
23. Bragg WL, Williams EJ(1934) The Effect of Thermal Agitation on Atomic Arrangement in Alloys. Proceedings of the Royal Society of London. Series A, Containing Papers of a Mathematical and Physical Character. **145**(855): p. 699-730.
24. Slaughter DW, Doherty MF (1995) Calculation of solid-liquid equilibrium and crystallization paths for melt crystallization processes. Chem Eng Sci 50(11): p. 1679-1694.
25. Abes M,Bouzidi L, Narine SS (2007) Crystallization and phase behavior of 1,3-propanediol esters II. 1,3-Propanediol distearate/1,3-propanediol dipalmitate (SS/PP) and 1,3-propanediol distearate/1,3-propanediol dimyristate (SS/MM) binary systems. Chemistry and Physics of Lipids **150**: p. 89-108.
26. Boodhoo MV, Kutek T, Filip V, Narine SS (2008) The binary phase behavior of 1,3-dimyristoyl-2-stearoyl-sn-glycerol and 1,2-dimyristoyl-3-stearoyl-sn-glycerol. Chemistry and Physics of Lipids **154**(1): p. 7-18.
27. Prausnitz JW, Lichtenthaler RN, Gomes de Azevedo E (1998) Molecular thermodynamics of fluid phase equilibria. 3th edn. Prentice-Hall, New York.
28. McDonald CM, Floudas CA (1997) GLOPEQ: A new computational tool for the phase and chemical equilibrium problem. Comp. Chem. Eng 21:1-23.
29. Teles dos Santos M, Carrilo Le Roux GA, Joulia X, Gerbaud V (2009) Solid-Liquid Equilibrium Modelling and Stability Tests for Triacylglycerols Mixtures. Computer Aided Chemical Engineering 27: 885-890.
30. Michelsen ML (1982) the isothermal flash problem. Part I. stability. Fluid Phase Equilibr 9: 1– 19.
31. Rosenthal RE (2008) GAMS Release 23.2. A User's Guide. GAMS Development Corporation, Washington, DC, USA.
32. Takiyama H, Suzuki H, Uchida H, Matsuoka M (2002) Determination of solid–liquid phase quilibrium by using measured DSC curves. Fluid Phase Equilibr 194–197: 1107–1117.
33. Zéberg-Mikkelsen CK, Stenby EH (1999) Predicting the melting points and the enthalpies of fusion of saturated triglycerides by a group Contribution method. Fluid Phase Equilibr 162: 7-17.
34. Ceriani R, Gani R, Meirelles AJA (2009) Prediction of heat capacities and heats of vaporization of organic liquids by group contribution methods. Fluid Phase Equilibr 28: 49–55.
35. Bruin S (1999) Phase equilibrium for food product and process design. Fluid Phase Equilibr 158–160: 657–671.
36. Sambanthamurthi R, Sundram K, Tan Y (2000) Chemistry and biochemistry of palm oil. *Progress in Lipid Research* 39:507 – 558.
37. Lin SW (2002) Palm Oil. In: Gunstone FD (ed) Vegetable Oils in Food Technology: Composition, Properties and Uses. Blackwell, Oxford, pp.59-97.
38. Keller G, Lavigne F, Loisel C, Ollivon M, Bourgaux C (1996) Investigation of the complex thermal behaviour of fats. J. Therm. Anal 47: 1545 – 1565.
39. Sato K, Koyano T (2001) Crystallization Properties of Cocoa Butter. In: Garti N, Sato K (eds) Crystallization Processes in Fats and Lipid Systems. Marcel Dekker, New York.pp.429-456.

CAPTIONS

Fig. 1: Number of triacylglycerols that can be formed from fatty acids (including optical and positional isomers).

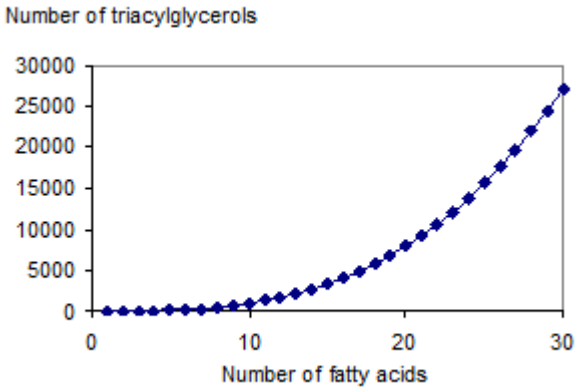

Fig. 2: Experimental and predicted phase diagram for mixture POP-PPP.

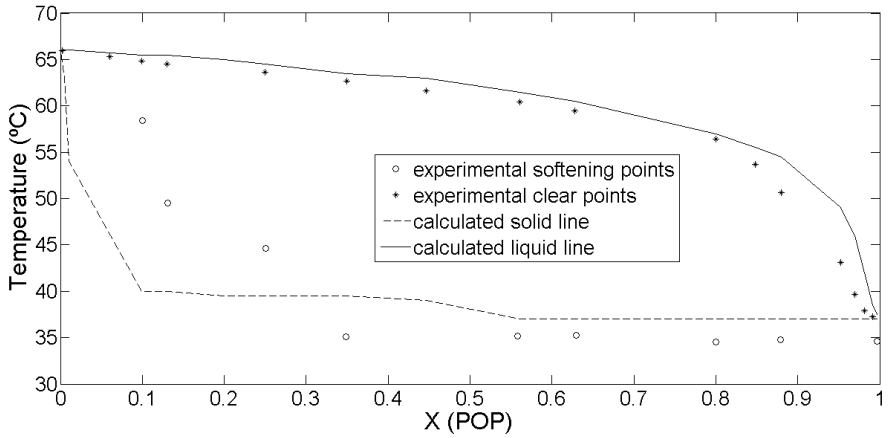

Fig. 3: Simulated SFC vs Temperature and simulated and experimental DSC for mixture MPM/SSO/OOO.

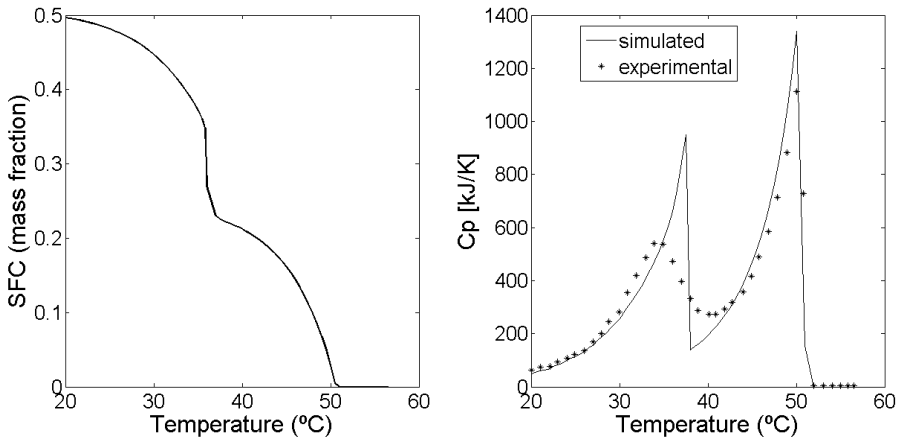

Fig. 4: Melting profile and DSC curve of palm oil.. Calculated: full lines. Experimental data: symbols [37].

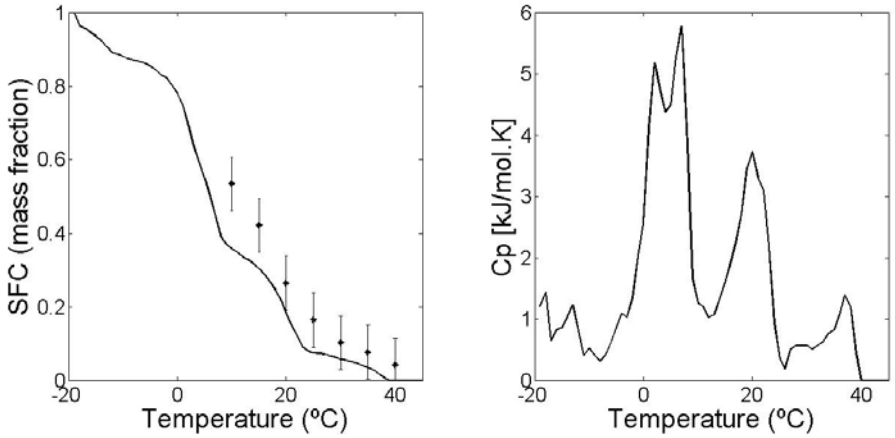

Fig. 5: Melting profile and DSC curve of cocoa butter. Calculated: full lines. Experimental data: symbols [20].

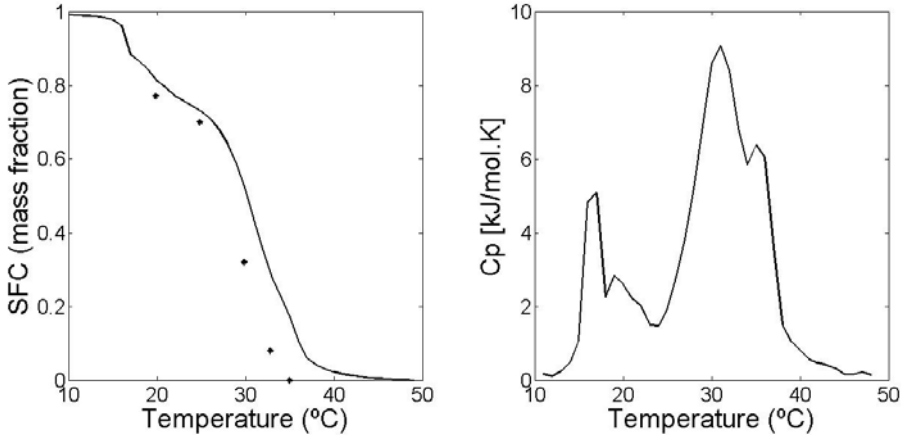

Fig. 6: Simulated melting curves for palm oil enriched with Caprylic-EPA-Caprylic structured lipid (different concentrations) compared with the melting curve for pure palm oil.

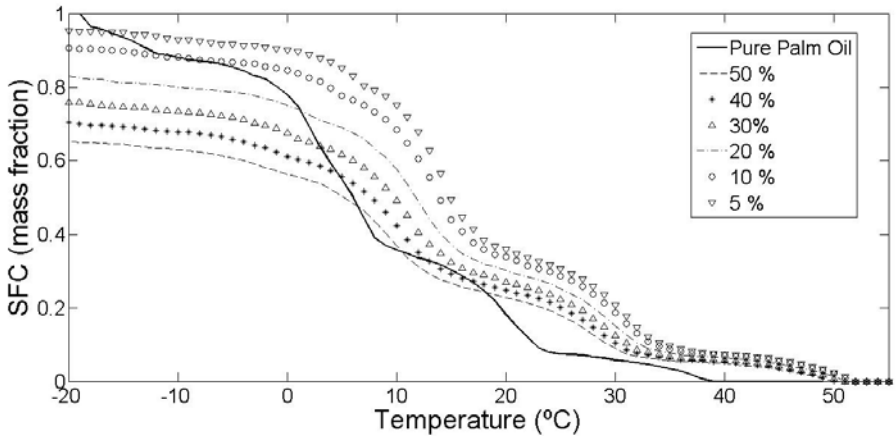

Fig. 7: Simulated DSC curves for the mixtures presented in Fig.6.

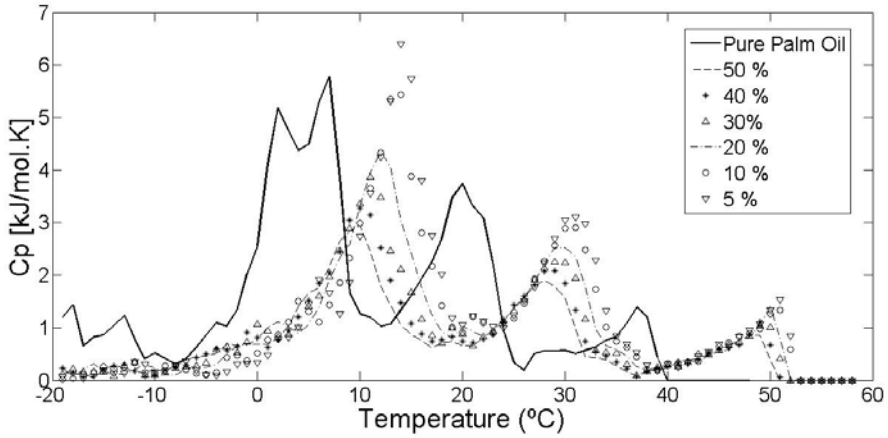

Fig. 8: Simulated Melting curves for palm oil enriched with different structured lipids.

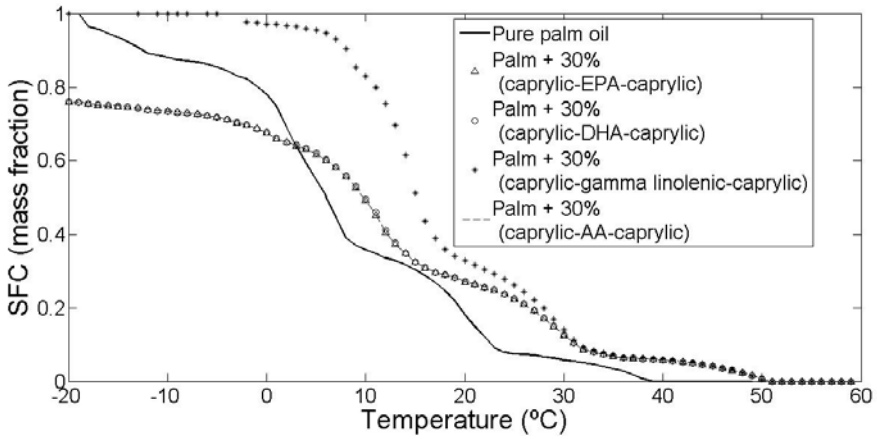

Fig. 9: Simulated DSC curves for the mixtures presented in Fig.8.

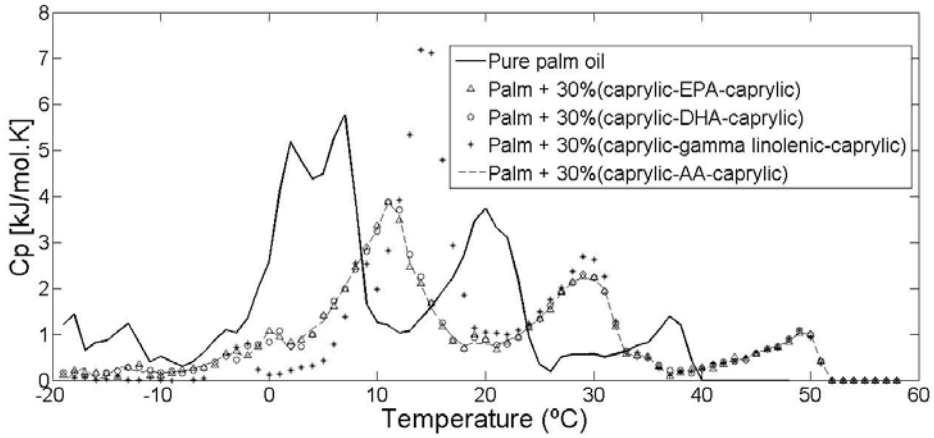

Table 1: Type of mixtures used.

Binary Mixture	Ternary Mixture	Multicomponent Mixtures (vegetable oils)	Blends of Vegetable Oils and Structured Lipids
POP/PPP	MPM/SSO/OOO	Palm Oil	Palm Oil + (Caprylic – EPA – Caprylic)
		Cocoa Butter	Palm Oil + (Caprylic - DHA – Caprylic)
			Palm Oil + (Caprylic – γ linolenic – Caprylic)
			Palm Oil + (Caprylic – AA – Caprylic)

P: palmitic acid (C16:0) O: oleic acid (18:1) M: myristic acid(C14:0) S: stearic acid (18:0)
EPA: eicosapentaenoic acid (C20:5) DHA: docosahexaenoic acid (C22:6)
AA:arachidonic acid (C20:4) γ- linolenic acid: 6,9,12-octadecatrienoic acid (C18:3).

Table 2: Weight fraction of Pure Palm Oil and Cocoa Butter.

Palm Oil [36]		Cocoa Butter [39]	
TAG	Mass Fraction (%)	TAG	Mass Fraction (%)
POO	20.54	POS	40.2
POP	20.02	SOS	21.7
PPO	7.16	POP	13.9
PPP	6.91	SOO	6.7
PLO	6.59	POO	5.8
PLP	6.36	PLS	3.9
OOO	5.38	PLP	1.7
POS	3.5	PLO	0.9
POL	3.39	OOO	0.7
OPO	1.86	PPS	0.6
SOO	1.81	SSS	0.6
OOL	1.76	PSS	0.5
OLO	1.71	-	-
PPS	1.21	-	-
PPL	1.17	-	-
PLS	1.11	-	-
PLL	1.08	-	-
Others	8.44		2.8
Total	**100**	**-**	**100**

P: palmitic; O: oleic; L: linoleic; S: stearic